

Impact of a Concha Bullosa on Nasal Airflow Characteristics in the Setting of Nasal Septal Deviation: A Computational Fluid Dynamics Analysis

American Journal of Rhinology & Allergy

2020, Vol. 34(4) 456–462

© The Author(s) 2020


Article reuse guidelines:

sagepub.com/journals-permissions

DOI: 10.1177/1945892420905186

journals.sagepub.com/home/ajr



Lifeng Li, MD¹ , Hongrui Zang, MD, PhD¹,
Demin Han, MD, PhD¹, Murugappan Ramanathan Jr, MD²,
Ricardo L. Carrau, MD, MBA³, and Nyall R. London Jr, MD, PhD^{2,4}

Abstract

Background: A concha bullosa (CB) of the middle turbinate is frequently observed on the nondeviated side of patients with a nasal septal deviation (NSD). However, the impact of the CB on nasal airflow characteristics in patients with NSD has been incompletely defined.

Objective: The purpose of this study was to evaluate the impact of a CB in patients with NSD on nasal airflow characteristics using a computational fluid dynamics (CFD) approach.

Methods: Twenty patients with NSD and a unilateral CB of the middle turbinate on the nondeviated side (study group) were recruited. Another 20 patients with NSD without the formation of a CB (control group) were also enrolled. Using CFD, the maximal airflow velocity, nasal resistance, maximal wall shear stress, and minimal temperature in the bilateral nostrils of each group were assessed. Moreover, the volume of the nasal tract, surface area-to-volume ratio, and the total nasal resistance were compared between the study and control groups.

Results: In the study group, no significant differences of airflow dynamics between the bilateral nasal cavities were observed. In the control group, however, there were statistically significant differences for maximal airflow velocity, nasal resistance, maximal wall shear stress, and minimal airflow temperature between the bilateral nostrils. The surface area-to-volume ratio and total nasal resistance in the study group was significantly higher and the nasal volume was significantly decreased than that in the control group.

Conclusion: CB of the middle turbinate on the nondeviated side of patients with NSD rendered airflow characteristics more evenly distributed between the bilateral nostrils as assessed by CFD. From an aerodynamics perspective, a CB may represent a compensatory action to normalize airflow dynamics. However, a CB may also result in constriction of the ipsilateral nasal cavity.

Keywords

nasal septal deviation, concha bullosa, aerodynamics, computational fluid dynamics

Introduction

A concha bullosa (CB), or pneumatized cavity of the middle turbinate, is common in patients with nasal septal deviation (NSD), especially on the nondeviated side.^{1–3} It is unclear, however, which develops first and whether the formation of a CB may be a compensatory result of NSD.^{4–6} Several studies have analyzed this relationship. Uygur et al. correlated the angle of NSD and degree of CB pneumatization and concluded that the

¹Department of Otolaryngology—Head and Neck Surgery, Beijing Tongren Hospital, Capital Medical University, Beijing, China

²Department of Otolaryngology—Head and Neck Surgery, Johns Hopkins School of Medicine, Baltimore, Maryland

³Department of Otolaryngology—Head and Neck Surgery, The James Cancer Hospital at the Wexner Medical Center of The Ohio State University, Columbus, Ohio

⁴National Institute on Deafness and Other Communication Disorders, National Institutes of Health, Bethesda, Maryland

Corresponding Author:

Nyall R. London Jr, Department of Otolaryngology—Head and Neck Surgery, Johns Hopkins School of Medicine, 6th Floor, 601 N. Caroline Street, Baltimore, MD 21287, USA.

Email: nlon2@jhmi.edu

NSD does not give rise to the formation of a CB but may augment the pneumatization of the middle turbinate dependent on the degree of the NSD angle.⁷ Stallman et al. have suggested that the NSD does not occur as a direct result of mass effect from the CB as air channels are preserved between the nasal septum and CB.⁴ Yigit et al. have also suggested that the increasing incidence of unilateral CB in patients with NSD, especially on the non-deviated side, implied that the septal deviation may prevent the development of CB on the deviated side.¹

The presence of a CB on the nondeviated side of patients with NSD may impact the nasal airflow physiology or restrict the ipsilateral volume of the nasal cavity. However, to the authors' knowledge, there are few studies evaluating the aerodynamic impact of a CB on nondeviated side in patients with NSD. Computational fluid dynamics (CFD) is an objective measurement to simulate airflow pressure and velocity distribution, wall shear stress, and airflow temperature in the nasal cavity and has become a popular method to assess nasal aerodynamics.^{8–13} We therefore hypothesized that a CB of the middle turbinate in patients with NSD could help maintain the relative aerodynamic balance between the bilateral nasal cavities and could potentially represent a compensatory action due to the wider cavity induced by septal deviation. The purpose of this study was to assess the impact of a CB of the middle turbinate on nasal airflow characteristics in patients with NSD using CFD analysis.

Material and Methods

Patient Enrollment

Eighty-two consecutive patients who had undergone computed tomography (CT) scanning of the nasal cavity and paranasal sinuses for septal deviation between January 2015 and December 2015 were evaluated. Among these subjects, 20 patients with an NSD and concurrent CB on the nondeviated nostril (Figure 1

(A)) were recruited for investigation and defined as the study group. Another 20 age- and sex-matched patients with NSD without the formation of CB (Figure 1(B)) were enrolled as the control group. CT evidence of sinusitis was observed in both the study group ($n = 5$) and the control group ($n = 4$). However, the patients with allergic rhinitis, pansinusitis, obvious polyps, and bilateral CB formation were excluded from the study. Informed consent was obtained from these 40 subjects, and the study protocol was approved by the Ethics Committee of Beijing Tongren Hospital.

CFD Analysis

CT scans combining the axial, coronal, and sagittal reconstructions were implemented. DICOM (Digital Imaging and Communications in Medicine) format images were obtained at a spatial resolution of 512×512 pixels and 0.625 mm thickness. Segmentation and primary smoothing of the raw images was conducted using Mimics 13.1 (Materialise, Leuven, Belgium). The Mimics models were then imported into Geomagic studio 12 (Geomagic, North Carolina, USA) for further smoothing and surface partition. This was followed by acquisition of surface elements of IGES (Initial Graphics Exchange Specification) format for meshing.

Meshing was performed in ICEM-CFD (The Integrated Computer Engineering and Manufacturing code for Computational Fluid Dynamics; ANSYS, Canonsburg, Pennsylvania), and global and local controls were taken to improve mesh quality. Meshes with the value of maximal skewness less than 0.6 were then imported into Fluent 13.0 (ANSYS) for solution procedures. To improve the accuracy of numerical simulation, mesh independent analysis was conducted in each individual to select the appropriate mesh number for final analysis.¹⁴

In CFD simulations, the flow was assumed to be incompressible and quasi-steady. Characteristic values for airflow and temperature fields were derived from the continuity, Navier–Stokes, and energy equations.

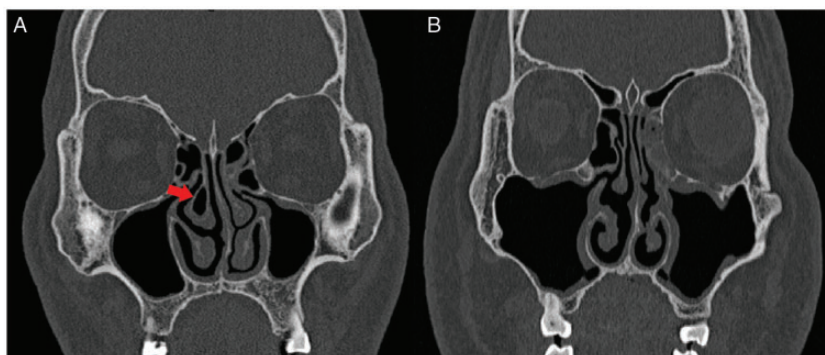


Figure 1. Coronal CT scans of representative cases. (A) Patient of NSD with the formation of CB (arrow, study group). (B) Patient of NSD without CB (control group).

The RNG (Renormalization Group) k -epsilon turbulence model was chosen for CFD simulation. SIMPLEC (Semi-Implicit Method for Pressure-Linked Equations Consistent) algorithm and second-order upwind format discretization of momentum, turbulent kinetic energy, turbulent dissipation rate, and energy were adopted.

Atmospheric pressure and 20°C were imposed on both nasal cavities. The nasal wall was assumed to be no-slip ($u = v = 0$) and isothermal (set at 34°C).¹⁵ A constant airflow rate of 15 L/min was applied to the anterior nostril as the flow rate for simulation.

Data processing was conducted in CFD-Post (ANSYS) to obtain contour visualization and numerical outputs. Indices such as maximal airflow velocity, nasal resistance, maximal wall shear stress, and minimal temperature (at the head of the middle turbinate) were compared between bilateral nostrils. Moreover, the nasal airflow volume, surface area-to-volume ratio, and total nasal resistance were also compared between the study and control groups.

Statistical Analysis

Differences of aerodynamic indices between bilateral nasal cavities within the study group and control group, and the aerodynamic indices of the respective nostril between the 2 groups were compared by t test.

Comparison of nasal airflow volume, surface area-to-volume ratio, and total nasal resistance between the study group and control group was conducted by the Mann-Whitney U test. The value was expressed as mean \pm standard deviation, and a probability value of $P < .05$ was considered to be statistically different. Statistical analysis was performed using the SPSS 16.0 software (StatSoft, Inc., Tulsa, Oklahoma).

Results

Nasal obstruction was the chief complaint, which occurred in the deviated side of all 20 patients (100%) in the control group. In the study group, however, the occurrence of nasal obstruction on the deviated side, nondeviated side and both sides were in 13 (65%), 2 (10%), and 5 (25%) patients, respectively.

In patients with NSD and CB of the nondeviated side, the airflow streamline (Figure 2(A)) was evenly distributed with no apparent difference of maximal airflow velocity between the deviated (4.42 ± 1.86 m/s) and nondeviated nasal cavity (4.15 ± 1.17 m/s; $P = .59$, Table 1). In patients of NSD without the formation of a CB, however, the maximal airflow velocity in the deviated side (4.89 ± 2.37 m/s; Figure 2(B), arrow) was statistically higher than that in the nondeviated side (3.87 ± 1.99 m/s; Figure 2(B), triangle; $P < .05$, Table 1).

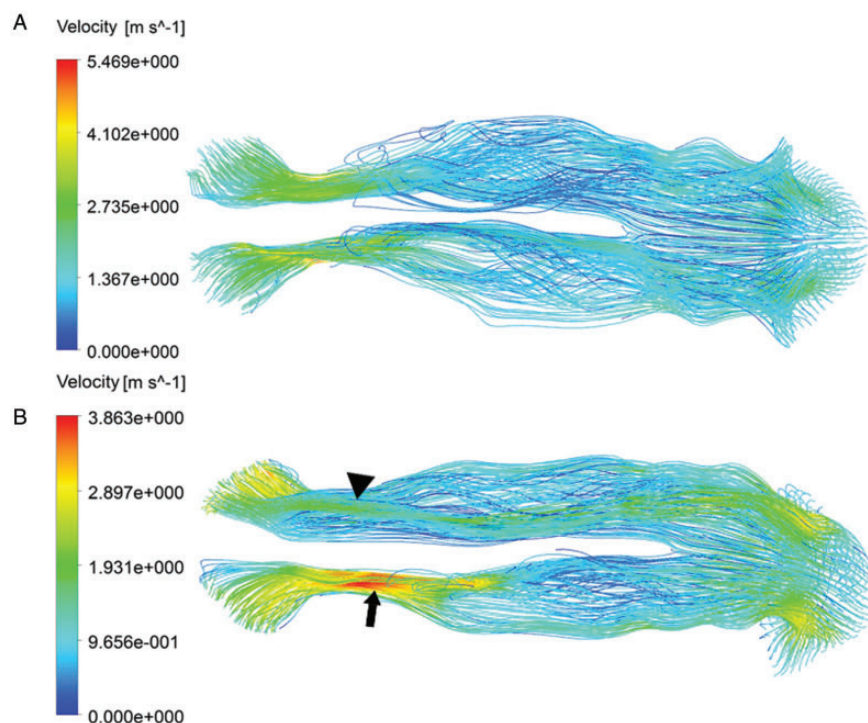


Figure 2. Airflow streamline distribution in bilateral nostrils. (A) Patient of NSD with the formation of CB, the airflow streamline is almost balanced between bilateral nostrils. (B) Patient of NSD without CB, the overall airflow velocity in deviated side (arrow) was obviously higher than that in nondeviated side (triangle).

Table 1. Comparison of MV (m/s), NR (kPa·s·L⁻¹), MWSS (Pa), and MT (at Head of Middle Turbinate, K) Between Bilateral Nostrils in SG and CG.

	MV			NR			MWSS			MT		
	D	ND	P	D	ND	P	D	ND	P	D	ND	P
SG	4.42 ± 1.86	4.15 ± 1.17	.59	0.23 ± 0.12	0.22 ± 0.11	.71	0.80 ± 0.43	0.75 ± 0.44	.7	301.52 ± 1.82	301.38 ± 1.60	.79
CG	4.89 ± 2.37	3.87 ± 1.99	.000	0.26 ± 0.05	0.10 ± 0.03	.000	0.86 ± 0.63	0.64 ± 0.48	.000	303.1 ± 2.70	299.89 ± 1.73	.000
P	.75	.000		.57	.000		.65	.000		.21	.19	

Abbreviations: CG, control group; D, deviated side; MT, minimal airflow temperature; MV, maximal airflow velocity; MWSS, maximal wall shear stress; ND, nondeviated side; NR, nasal resistance; SG, study group.

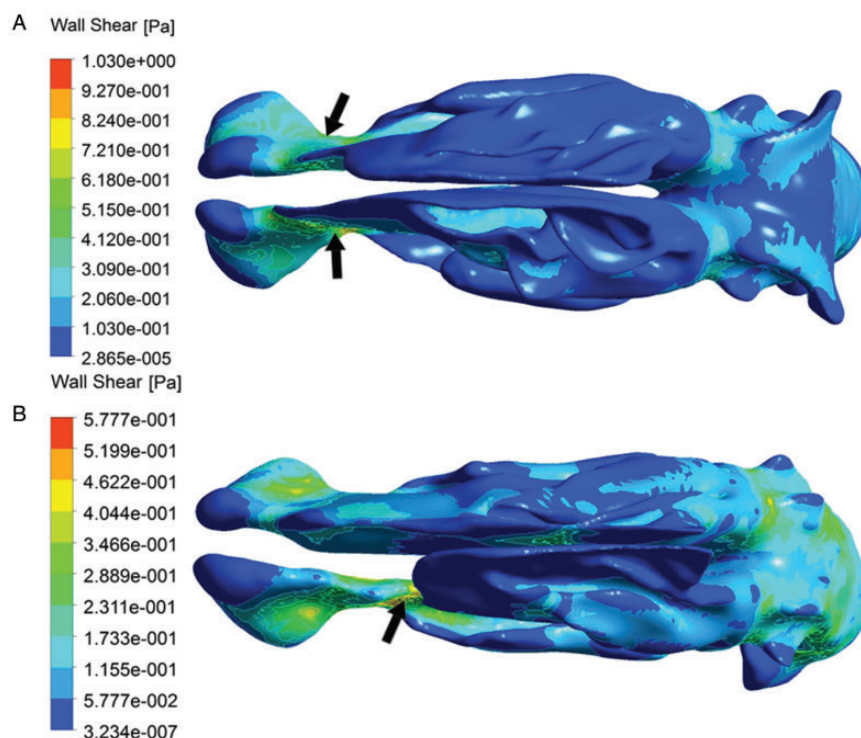


Figure 3. The contour of wall shear stress. (A) Patient of NSD with the formation of CB, the higher value was located near the nasal valve area (arrows) and no evident difference of wall shear stress distribution between bilateral nostril sides. (B) Patient of NSD without CB, the overall wall shear stress in deviated side was higher than that in nondeviated side, and the location of maximal wall shear stress in deviated side was also transferred (arrow).

In patients with NSD and CB, the maximal wall shear stress in both nostrils was identified to locate near the nasal valve area (Figure 3(A), arrows), and no evident difference of wall shear stress distribution between bilateral nasal cavities could be derived ($P = .7$, Table 1). In patients of NSD without the formation of a CB, however, the maximal wall shear stress on the deviated side (0.86 ± 0.63 Pa) was statistically higher than that in nondeviated side (0.64 ± 0.48 Pa; $P < .05$, Table 1). The maximal wall shear stress located near the nasal valve area on deviated side in 9 patients (45%). However, the location of maximal wall shear stress on deviated side

was detected to transfer to the posterior segment of nasal cavity (Figure 3(B), arrow) in the remaining 11 patients (5 around the head of inferior turbinate, 3 in the common meatus, and 3 close to the head of middle turbinate). For comparison of the location of maximal wall shear stress distributed on deviated sides in both the study and control groups, significant difference could be derived ($P = .001$).

In patients with NSD with the formation of CB, airflow temperature was evenly distributed between bilateral nasal cavities (Figure 4(A); $P = .79$, Table 1). In patients with NSD devoid of a CB, however,

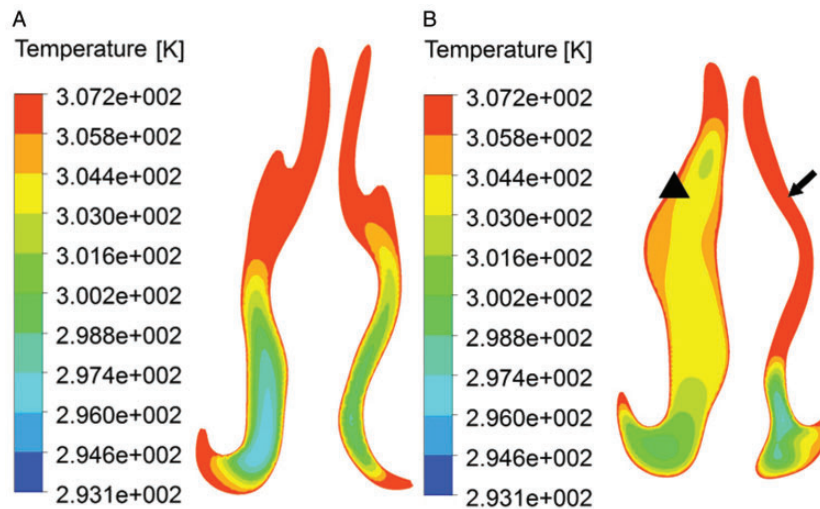


Figure 4. Temperature contour at level of head of middle turbinate. (A) Patient of NSD with the formation of CB, airflow temperature was evenly distributed between bilateral nostrils. (B) Patient of NSD without CB, the airflow temperature in deviated side (arrow) was higher than that in nondeviated side (triangle).

the minimal airflow temperature at the head of middle turbinate in the deviated side (303.1 ± 2.70 K; Figure 4 (B), arrow) was statistically higher than that in the non-deviated side (299.89 ± 1.73 K; Figure 4(B), triangle).

For comparison of airflow indices of the respective deviated and nondeviated sides between the study and control groups, significant difference of maximal airflow velocity, nasal resistance, and maximal wall shear stress could be derived in the nondeviated side ($P < .001$) but not in the deviated side ($P > .05$; Table 1). For minimal airflow temperature at head of middle turbinate, however, no significant difference existed in both the nondeviated and deviated sides ($P > .05$, Table 1).

The surface area-to-volume ratio (6.14 ± 0.75 cm⁻¹) and total nasal airway resistance (0.22 ± 0.13 kPa·s·L⁻¹) in the study group were statistically higher than that in the control group (5.72 ± 1.01 cm⁻¹, 0.19 ± 0.10 kPa·s·L⁻¹; $P < .05$, Table 2). However, the nasal airflow volume in the study group (30.16 ± 6.15 cm³) was statistically lower than that in control group (32.02 ± 7.49 cm³; $P < .05$, Table 2).

Discussion

The presence of a CB on the nondeviated side of patients with NSD is common.^{16,17} In this regard, the “e vacuo” phenomenon has been previously proposed to explain this occurrence.¹ The pneumatization of the middle turbinate may therefore be augmented in response to airflow changes as a result of the NSD. The study presented here investigated the alteration of aerodynamics characteristics in NSD patients with and without CB, which

Table 2. Comparison of the Nasal Volume (cm³), Surface Area-to-Volume Ratio (cm⁻¹) and Total Nasal Resistance (kPa·s·L⁻¹) Between the Study Group and Control Group.

	Study Group	Control Group	P
Nasal volume	30.16 ± 6.15	32.02 ± 7.49	.000
Surface area-to-volume ratio	6.14 ± 0.75	5.72 ± 1.01	.000
Total nasal resistance	0.22 ± 0.13	0.19 ± 0.10	.000

may improve our understanding of the correlation between CB and NSD.

Airflow velocity and wall shear stress are objective measurements to assess the main airflow characteristics of the nasal cavity.^{12,13} The location of maximal wall shear stress often indicates the narrowest site of the ipsilateral nasal cavity, which mainly locates at the nasal valve area.^{18,19} Through CFD analysis presented in this study, the main aerodynamic indices in the deviated side were significantly different from that in nondeviated side in control group. The transfer of the location of maximal wall shear stress into the posterior nasal cavity in the control group may indicate that the narrowest site was altered due to the action of NSD. In the study group, however, the relative balance of the wall shear stress between bilateral nostrils was maintained. This may therefore suggest that the formation of CB can help keep the airflow balance between bilateral nostrils in patients with NSD.

Furthermore, the minimal airflow temperature at the head of middle turbinate reflects the warming capacity of the nasal cavity,^{8,18} which was often adopted to assess

the warming function of the nasal cavity.²⁰ In this study, significant difference of minimal airflow temperature between bilateral nostrils could be detected in control group but not in study group. Of note, when comparing the minimal airflow temperature in the respective deviated and nondeviated sides between the 2 groups, no significant difference could be derived. The resultant outcomes may therefore imply that the existence of CB in the nondeviated side can help maintain the balance of warming capacity between bilateral nostrils; however, the overall impact of the NSD on warming capability was limited, which is also in accordance with our previous study.¹⁹

Yu et al. demonstrated that the nasal cavity has the capacity of self-adaptation following structural alterations.²¹ The fluid experiments in NSD models implemented by Grützmacher et al. demonstrated that the formation of a “low-velocity area” on the nondeviated side was defined as “dead space.”²² The relatively decreased airflow velocity, wall shear stress, and decreased warming capacity on the nondeviated side of patients with NSD without the formation of CB may contribute to proliferation of the lateral nasal wall to maintain the normal nasal physiology.²² This mainly manifested as hypertrophy of the inferior turbinate or pneumatization of the middle turbinate. In this study, the aerodynamic difference between bilateral nostrils disappeared when the CB coexisted in the nondeviated side of patients with NSD. According to the aerodynamics results derived from this study, the CB on nondeviated side of patients with NSD could potentially represent an example of evolutionary self-adaptation.

The surface area-to-volume ratio and nasal airflow volume are considered to be useful measurements to determine whether a nasal cavity is narrow or wide.^{21,23} The narrower the cavity, the larger the area volume ratio, and vice versa.^{24,25} The increased surface area-to-volume ratio and reduced nasal volume in patients with NSD with the formation of CB indicated that the ventilation may be further limited due to the more constricted cavity by comparison with patients with NSD without the formation of CB,²⁶ which may provide the explanation for that the nasal obstruction occurred in nondeviated or both sides in a portion of patients in study group.

In addition, nasal resistance is another objective index to assess the ventilation capacity of the nasal cavity.²⁷ In the control group, the nasal resistance in the deviated side was significantly higher than that in the nondeviated side. In the study group, however, no significant difference of nasal resistance between the bilateral nostrils was identified. However, the total nasal resistance in patients of the study group was significantly increased in comparison with patients in control group. It also implies

that the nasal cavity became more constricted in patients of NSD with the formation of a CB.

There are also limitations to this study. It is a computational simulation study, and the resultant outcomes need to be further validated in patients. Moreover, the effect of structural factors on airflow characteristics is complicated, which may incorporate multiple variables (ie, nasal cycle, constriction of the nasal valve region, hypertrophy of inferior turbinate, inflammation status of the nasal mucosa, existence of CB, or inverse middle turbinate) and needs to be further investigated. Furthermore, assessment with respect to the location and severity of NSD, and the volume of CB was not incorporated in this study, which would also deserve further investigation to enhance appreciation of aerodynamic alterations with variable extent of structural abnormalities.

Conclusion

CB on the nondeviated side of patients with NSD make the airflow characteristics more balanced between bilateral nasal cavities. From the perspective of aerodynamics, it may be a compensatory action for nasal physiology. However, the presence of CB narrowed the ipsilateral nasal cavity as assessed by nasal cavity volume, area volume ratio, and nasal resistance.

Declaration of Conflicting Interests

The author(s) declared the following potential conflicts of interest with respect to the research, authorship, and/or publication of this article: N. R. L. was a consultant for Cooltech Inc. and holds stock in Navigen Pharmaceuticals. All other authors declare no relevant conflicts of interest.

Funding

The author(s) received no financial support for the research, authorship, and/or publication of this article.

ORCID iD

Lifeng Li  <https://orcid.org/0000-0002-0114-7608>

References

1. Yigit O, Acioglu E, Cakir ZA, Sisman AS, Barut AY. Concha bullosa and septal deviation. *Eur Arch Otorhinolaryngol*. 2010;267:1397–1401.
2. Smith KD, Edwards PC, Saini TS, Norton NS. The prevalence of concha bullosa and nasal septal deviation and their relationship to maxillary sinusitis by volumetric tomography. *Int J Dent*. 2010;2010:404982.
3. Neskey D, Eloy JA, Casiano RR. Nasal, septal, and turbinate anatomy and embryology. *Otolaryngol Clin North Am*. 2009;42:193–205, vii.

4. Stallman JS, Lobo JN, Som PM. The incidence of concha bullosa and its relationship to nasal septal deviation and paranasal sinus disease. *AJNR Am J Neuroradiol*. 2004;25:1613–1618.
5. Ural A, Kanmaz A, Inancli HM, Imamoglu M. Association of inferior turbinate enlargement, concha bullosa and nasal valve collapse with the convexity of septal deviation. *Acta Otolaryngol*. 2010;130:271–274.
6. Arslan G, Karaali K. Concha bullosa and nasal septal deviation. *AJNR Am J Neuroradiol*. 2005;26:1882; author reply 1882.
7. Uygun K, Tuz M, Dogru H. The correlation between septal deviation and concha bullosa. *Otolaryngol Head Neck Surg*. 2003;129:33–36.
8. Li L, Han D, Zhang L, et al. Impact of nasal septal perforations of varying sizes and locations on the warming function of the nasal cavity: a computational fluid-dynamics analysis of 5 cases. *Ear Nose Throat J*. 2016;95: E9–E14.
9. Rhee JS, Pawar SS, Garcia GJ, Kimbell JS. Toward personalized nasal surgery using computational fluid dynamics. *Arch Facial Plast Surg*. 2011;13:305–310.
10. Li L, Han D, Zhang L, et al. Aerodynamic investigation of the correlation between nasal septal deviation and chronic rhinosinusitis. *Laryngoscope*. 2012;122:1915–1919.
11. Keck T, Lindemann J. Simulation and air-conditioning in the nose. *Laryngorhinootologie*. 2010;89 Suppl 1:S1–S14.
12. Chen XB, Lee HP, Chong VF, Wang de Y. Assessment of septal deviation effects on nasal air flow: a computational fluid dynamics model. *Laryngoscope*. 2009;119:1730–1736.
13. Maza G, Li C, Krebs JP, et al. Computational fluid dynamics after endoscopic endonasal skull base surgery—possible empty nose syndrome in the context of middle turbinate resection. *Int Forum Allergy Rhinol*. 2019;9:204–211.
14. Lee J-H, Na Y, Kim S-K, Chung S-K. Unsteady flow characteristics through a human nasal airway. *Respir Physiol Neurobiol*. 2010;172:136–146.
15. Lindemann J, Keck T, Wiesmiller K, et al. A numerical simulation of intranasal air temperature during inspiration. *Laryngoscope*. 2004;114:1037–1041.
16. Sazgar AA, Massah J, Sadeghi M, Bagheri A, Rasool E. The incidence of concha bullosa and the correlation with nasal septal deviation. *B-ENT*. 2008;4:87–91.
17. Hatipoglu HG, Cetin MA, Yuksel E. Nasal septal deviation and concha bullosa coexistence: CT evaluation. *B-ENT*. 2008;4:227–232.
18. Li L, London NR Jr, Zang H, Han D. Impact of posterior septum resection on nasal airflow pattern and warming function. *Acta Otolaryngol*. 2020;140:51–57. doi:10.1080/00016489.2019.1688388
19. Li L, Zang H, Han D, London NR Jr. Impact of varying types of nasal septal deviation on nasal airflow pattern and warming function: a computational fluid dynamics analysis [published online ahead of print September 30, 2019]. *Ear Nose Throat J*. 2019;145561319872745. doi:10.1177/0145561319872745
20. Lindemann J, Leiacker R, Rettinger G, Keck T. Nasal mucosal temperature during respiration. *Clin Otolaryngol Allied Sci*. 2002;27:135–139.
21. Yu S, Liu Y, Sun X, Li S. Influence of nasal structure on the distribution of airflow in nasal cavity. *Rhinology*. 2008;46:137–143.
22. Grützenmacher S, Robinson DM, Grafe K, Lang C, Mlynski G. First findings concerning airflow in noses with septal deviation and compensatory turbinate hypertrophy—a model study. *ORL J Otorhinolaryngol Relat Spec*. 2006;68:199–205.
23. Lindemann J, Tsakiropoulou E, Keck T, Leiacker R, Wiesmiller KM. Nasal air conditioning in relation to acoustic rhinometry values. *Am J Rhinol Allergy*. 2009;23:575–577.
24. Zhu JH, Lee HP, Lim KM, Lee SJ, Wang de Y. Evaluation and comparison of nasal airway flow patterns among three subjects from Caucasian, Chinese and Indian ethnic groups using computational fluid dynamics simulation. *Respir Physiol Neurobiol*. 2011;175:62–69.
25. Garcia GJ, Bailie N, Martins DA, Kimbell JS. Atrophic rhinitis: a CFD study of air conditioning in the nasal cavity. *J Appl Physiol*. 2007;103:1082–1092.
26. Paksoy M, Sanli A, Evren C, et al. The role of concha bullosa in nasal pathologies. *Kulak Burun Bogaz Ihtis Derg*. 2008;18:238–241.
27. Moore M, Eccles R. Objective evidence for the efficacy of surgical management of the deviated septum as a treatment for chronic nasal obstruction: a systematic review. *Clin Otolaryngol*. 2011;36:106–113.